PHYSICAL REVIEW B VOLUME 18, NUMBER 11 1 DECEMBER 1978

# Nuclear-magnetic-resonance study of $Li^+$ motion in lithium aluminates and LiOH

D. M. Follstaedt and R. M. Biefeld
*Sandia Laboratories, Albuquerque, New Mexico 87185*
(Received 20 March 1978)

We report $T_1$ and $T_2$ measurements of $^7Li$ resonances, which demonstrate thermally activated motion of $Li^+$ in the ionic conductors $\alpha$- and $\beta$-$Li_5AlO_4$. At high temperatures our data give $T_1/T_2 \approx (I+1/2)^2 = 4$, which demonstrates that dipole interactions between magnetic impurities and $^7Li$ produce the relaxation, even for our nominally pure samples, which are shown by ESR measurements to contain $\sim 15$-ppm magnetic impurities. A liquidlike spatial diffusion model is used to analyze the relaxation times. At high temperatures the relaxation is determined by the $Li^+$ jump time for which our analysis gives an activation energy $E_a = 0.83(2)$ eV for $\alpha$, and $E_a = 0.56(4)$ eV for $\beta$, with an attempt frequency $\nu_0 = 2 \times 10^{12}$ sec$^{-1}$ for both phases. Near room temperature, $T_1$ is apparently determined by the impurity relaxation time, for which we estimate $T_{1e} \sim 10^{-5}$ sec. $T_2$ measurements in LiOH show motional narrowing of the $^7Li$ resonance above 320°C but not the $^1H$ resonance, and thus identify $Li^+$ as the conducting ion in LiOH. Limited $T_1$ and $T_2$ measurements are also reported for $^7Li$ in $\gamma$-$LiAlO_2$.

## I. INTRODUCTION

Solid-state ionic conductors are of technological interest for a variety of possible applications such as high-energy density storage batteries. $Li^+$ conductors are receiving special attention because of the low atomic weight of Li and its large reduction potential. Among the most promising candidates for a $Li^+$ conductor at ~450 °C is $Li_5AlO_4$, for which Raistrick *et al.*[1] obtained conductivities as high as 0.3 $(\Omega\,\mathrm{cm})^{-1}$. To learn more about its conduction mechanism, we began work on $Li_5AlO_4$. Johnson *et al.*[2] have since shown that the reported high conductivities can be obtained only by exposing pure samples to water vapor, or by initially incorporating excess LiOH in the samples. This paper reports our work on pure $\alpha$- and $\beta$-$Li_5AlO_4$ and a limited investigation of LiOH. Further work on composite samples is underway at our laboratory. A discussion of the crystal structure and thermal properties of $Li_5AlO_4$ is given in Sec. II.

We have used pulsed NMR to probe the diffusion of $Li^+$ in our samples. Nuclear relaxation occurs by fluctuations in the local environment of the nucleus, and hence can be sensitive to diffusion processes. We have measured the transverse relaxation rate ($T_2^{-1}$) and the longitudinal or spin-lattice relaxation rate ($T_1^{-1}$) of the $^7Li$ nuclei in our samples. In Sec. III we define these relaxation rates more precisely and discuss their experimental determination. Because the $^7Li$ nucleus has spin $I(^7Li) = \frac{3}{2}$, it possesses an electric quadrupole moment and interacts with electric field gradients in its vicinity. The consequences of this interaction on $T_1^{-1}$ and $T_2^{-1}$ are also given in Sec. III.

Our initial attempts to prepare $Li_5AlO_4$ resulted in the $\beta$ phase being quenched into a metastable state. Since the data from this phase demonstrate diffusion-governed relaxation rates, we present the $T_1^{-1}$ and $T_2^{-1}$ results in Sec. IV A. The ratio $T_1/T_2$ at high temperatures is found to agree with that calculated for dipolar interactions with magnetic impurities, while disagreeing with the calculated ratio for electric quadrupole interactions. We present a liquid like diffusion model which accounts for our $\beta$-$Li_5AlO_4$ data quite well, and extract the activation energy and attempt frequency of the $Li^+$ jump responsible for $^7Li$ relaxation. We also identify a temperature regime where fluctuations of the impurity moment determine $^7Li$ relaxation, instead of $Li^+$ jumps.

Our initial $\beta$-$Li_5AlO_4$ samples were found to contain $\gamma$-$LiAlO_2$. To separate the signals of the two components in relaxation curves, $^7Li$ data were obtained on pure $\gamma$-$LiAlO_2$. The limited results are presented in the Appendix since they also demonstrate some of the diffusive features found in $Li_5AlO_4$.

$\alpha$-phase data similar to $\beta$ are presented in Sec. V. Although $T_1^{-1}$ does not exhibit the dependence on the nuclear-resonance frequency expected from the diffusion model, we use it to extract the jump attempt frequency and activation energy.

To investigate the conduction mechanism of LiOH, whose presence so radically alters the conductivity of $Li_5AlO_4$ samples, we have measured its $^7Li$ and $^1H$ relaxation rates. Unfortunately, $T_1^{-1}$ is much less experimentally accessible than in the above compounds. Thus we report only $T_2^{-1}$ data in Sec. VI. These data clearly identify $Li^+$ as the conducting ion.

In Sec. VII, we discuss possible explanations for deviations of the data from the theoretical model given in Sec. IV A. None are found to be

 

entirely satisfactory. We examine the jump parameters obtained for $\alpha$- and $\beta$-$Li_5AlO_4$. Finally, we discuss the distinguishing features of relaxation by magnetic impurities and examine nuclear relaxation in other ionic conductors where such relaxation may be dominant.

## II. PROPERTIES OF $Li_5AlO_4$

### A. Structural description

$Li_5AlO_4$ exists in either a low-temperature ($\alpha$) or high-temperature ($\beta$) structure with the $\alpha$ to $\beta$ transition occurring at ~780 °C. Detailed structural determinations have been carried out on both $\alpha$- and $\beta$-$Li_5AlO_4$.[3-5] The structure of isotopic $\alpha$-$Li_5GaO_4$ has also been reported.[6] These structures are ordered derivatives of the antifluorite ($Li_2O$) structure with vacancies occupying distinct lattice positions and can be formulated as $Li_5V_2AlO_4$ where $V$ represents a vacancy.

$\alpha$-$Li_5AlO_4$ crystallizes in the orthorhombic space group $Pbca$ with $a = 9.087$, $b = 8.947$, and $c = 9.120$ Å and with eight formula units in the unit cell.[6] The Li and Al atoms and the vacancies occupy the tetrahedral sites in the nearly fcc array of O atoms. Their ordered arrangement and their slight displacements from the ideal antifluorite positions give rise to the orthorhombic rather than cubic structure. These atoms and the vacancies occupy the general (8$c$) positions. There are five crystallographically distinct Li atom positions giving rise to a total of 40 Li atoms in the unit cell. Although each Li atom has identical nearest neighbors, each being tetrahedrally coordinated by four oxygen atoms, they have different next-nearest and further-distant neighbors. These differences can in principle cause the five distinct types of Li atoms to have different activation energies or potential barriers for motion. Also, there are three distinct types of empty octahedral positions in the fcc oxygen atom array. If the lithium ion motion were to take place through the octahedral positions, there could again be different activation energies for motion.

$\beta$-$Li_5AlO_4$ crystallizes in the orthorhombic space group $Pmmn$ with $a = 6.420$, $b = 6.302$, and $c = 4.620$ Å with two formula units in the unit cell.[4,5] Again the Li and Al atoms and the vacancies occupy tetrahedral sites and their ordered arrangement causes the orthorhombic distortion from cubic symmetry. There are two distinct Li atom positions, one in the general (8$g$) position and one in the special (2$b$) position. Also, there are two slightly different octahedral positions. Either of these differences could cause more than one activation energy for motion of the Li atoms.

### B. Materials preparation

Reagent grade $Li_2O$ and $Al_2O_3$ were used to prepare both $\alpha$- and $\beta$-$Li_5AlO_4$. The supplier's specifications give ~10-ppm Fe content, a significant point since we shall show that the $^7Li$ relaxation is due to dilute magnetic impurities. To prepare $\alpha$-$Li_5AlO_4$ from these materials, they were heated at 650 °C in alumina crucibles in air or $O_2$ for 2–6 days. Samples of $\beta$-$Li_5AlO_4$ were prepared by melting the $\alpha$-$Li_5AlO_4$ powder in an alumina crucible at ~1100 °C and then annealing at 900 °C for ~24 h. After the annealing period at 900 °C the high-temperature structure, $\beta$-$Li_5AlO_4$, was retained by quenching the sample. Both $\alpha$- and $\beta$-$Li_5AlO_4$ samples were stored in an argon filled glove box to prevent hydration. The NMR measurements were carried out on samples sealed in quartz tubes under a partial atmosphere of argon or vacuum to avoid contamination by water vapor.

## III. NUCLEAR RELAXATION FOR $I = \frac{3}{2}$

To more clearly identify $T_1^{-1}$ and $T_2^{-1}$, we need to discuss the properties of the $^7Li$ nuclear resonance and the manner in which the relaxation rates are measured. An important feature of the $^7Li$ resonance is that the nucleus has spin $I$ ($^7Li$) $= \frac{3}{2}$ and has an electric quadrupole moment. The four evenly spaced energy levels of an isolated nucleus in a magnetic field are perturbed by the electric field gradient of the surrounding ions in the solid. The $\pm\frac{3}{2} \rightleftharpoons \pm\frac{1}{2}$ nuclear transitions are shifted in frequency from the unshifted (in a first order perturbation treatment) $+\frac{1}{2} \rightleftharpoons -\frac{1}{2}$ transition, which alone is observed in our experiments. This has important consequences for $T_1^{-1}$ and $T_2^{-1}$ measurements.

$T_1^{-1}$ is measured as follows. A "comb" of 8–10 saturating pulses is applied at the resonance frequency to destroy the net nuclear magnetization of the resonance. After a delay time $t_d$ from the last comb pulse, the nuclear magnetization is measured by the spin-echo amplitude. The magnetization $M(t_d)$ for simple $I = \frac{1}{2}$ systems recovers as

$$M(t_d) = M(\infty)(1 - e^{-t_d/T_1}) . \quad (1)$$

Thus, one expects a linear plot for the quantity $\ln[1 - M(t_d)/M(\infty)]$ vs $t_d$, with slope $T_1^{-1}$.

However because of the quadrupole splitting of the $^7Li$ nuclear transitions, the magnetization recovery can relax as a sum of several exponential terms. This can occur even when the quantum mechanical process causing the nuclear relaxation is a $\Delta m = \pm 1$ process,[7,8] as is the case for magnetic impurities. For $I(^7Li) = \frac{3}{2}$, we would then

expect the plotted quantity to then decay as

$$ae^{-t_d/T_1}+be^{-6t_d/T_1}, \quad (2)$$

where $a+b=1$. In such systems, one finds that the $b$ term can be minimized by optimizing the comb pulse width, adding more pulses, and spacing the comb pulses $\sim T_2$ apart. Experimentally we find that the slow component can be made to exceed $a>0.8$ and often 0.9, and take its slope to be $T_1^{-1}$.

By $T_2^{-1}$ we mean the phase-memory decay rate. In most cases, we observe the resonance by using two equal width rf pulses separated by time $t$ to generate a spin echo at time $2t$ after the first pulse. $T_2^{-1}$ is then obtained by measuring the decay of the echo amplitude with pulse spacing, which goes as $e^{-2t/T_2}$. $T_2^{-1}$ thus measured corresponds to the homogeneous broadening of the nuclear resonance linewidth and not the full width with inhomogeneous broadening.

Effects due to observing only the $\frac{1}{2} \leftrightarrow -\frac{1}{2}$ transition can also be observed in the phase-memory decay rate when nonsecular (or lifetime, $T_1^{-1}$) contributions to $T_2^{-1}$ become significant. These contributions can be enhanced above the value of $\frac{1}{2}T_1^{-1}$, which applies for $I=\frac{1}{2}$ and for cases where all nuclear transitions occur at the same frequency. However, the enhancement for $+\frac{1}{2} \leftrightarrow -\frac{1}{2}$ depends upon the detailed form of the interaction producing the relaxation. In isotropic limits (where $T_1/T_2=1$ for $I=\frac{1}{2}$ for a dipolar interaction with a time-dependent local field

$$H_{\text{int}} = -\gamma_n \vec{I} \cdot \vec{H}_{\text{loc}}(t), \quad (3)$$

the ratio becomes[9]

$$T_1/T_2=(I+\tfrac{1}{2})^2, \quad (4)$$

which equals 4 for $I=\frac{3}{2}$. However for relaxation by the quadrupole interaction with a time-dependent electric field gradient, the same ratio has been calculated to be 1 for $I=\frac{3}{2}$.[10] Thus the two interactions can be distinguished in the isotropic limit.

## IV. METASTABLE $\beta$-$Li_5AlO_4$ DATA AND ANALYSIS

$T_1^{-1}$ and $T_2^{-1}$ data are shown for $\beta$-$Li_5AlO_4$ in Fig. 1 as a function of $T^{-1}$ ($K^{-1}$) for temperatures from room temperature (~24 °C) to 500 °C for frequencies of 7.2, 12.7, and 21.5 MHz. We attempted to take data above 500 °C, but samples cycled to higher temperatures would not reproduce $T_1$ values initially obtained below 500 °C, and also exhibited deterioration of their signal amplitudes. X-ray analysis of such samples showed the presence of the $\alpha$ phase. The $\beta$ phase can be "quenched in" from samples prepared at high temperatures

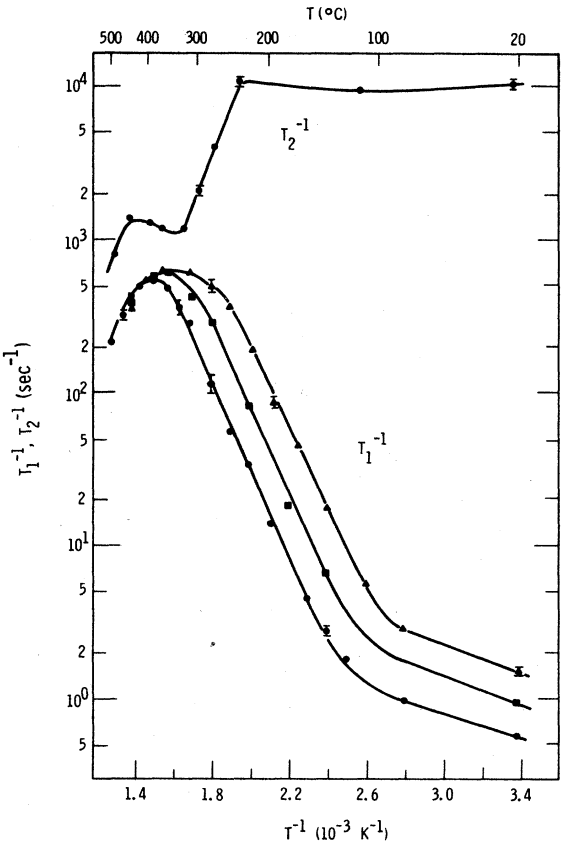


FIG. 1. Experimental values of $T_1^{-1}$ (●: 21.5 MHz, ■: 12.7 MHz, and ▲: 7.2 MHz) and $T_2^{-1}$ (●: 21.5 MHz) are given for the $^7$Li resonance in metastable $\beta$-$Li_5AlO_4$. Representative error limits are shown for selected points. The solid curves show experimental trends and are not theoretical fits to the data.

(>800 °C) where $\beta$ is the equilibrium phase, but on heating the sample to the range 500–800 °C, it evidently changes structure to the equilibrium phase of that temperature range $\alpha$. Thus data were not accepted for temperatures greater than 500 °C, nor from samples which had been cycled above this temperature. Since the data shown in Fig. 1 were reproducible after thermal cycling below 500 °C, and since they show a continuous temperature dependence, we accept them as valid data on a unique structure, metastable $\beta$-$Li_5AlO_4$.

Our initial $\beta$ samples showed two signal components in both transverse and longitudinal relaxation curves. We were able to identify the long $T_1$ component with the short $T_2$ component, and vice versa. X-ray examination of these samples detected the presence of $\gamma$-$LiAlO_2$. This led to our brief investigation of $\gamma$-$LiAlO_2$, which is presented in the Appendix. The $\gamma$-$LiAlO_2$ data are consistent with the long-$T_1$–short-$T_2$ values observed in the two-phase samples. Subsequently,

we were able to prepare samples consisting entirely of $\beta$-$Li_5AlO_4$, with $T_1$ and $T_2$ values consistent with the short-$T_1$–long-$T_2$ data mentioned above. Most of the data in Fig. 1 were obtained with these single-phase samples.

### A. Diffusive relaxation

$T_1^{-1}$ data above 146 °C and $T_2^{-1}$ above 236 °C show diffusive behavior. On the semilog plot in Fig. 1, $T_1^{-1}$ goes through a maximum at ~450 °C, with strong frequency dependence ($T_1^{-1} \propto \omega^{-1.8}$) on the low-temperature side of the maximum. $T_2^{-1}$ shows motional narrowing, with approximately the same activation energy [0.63(5) eV] as found in the $T_1^{-1}$ data [0.56(4) eV]. These features show that a Bloembergen-Purcell-Pound-type model[11] for relaxation by thermally activated diffusion (which gives $T_1^{-1} \propto \omega^{-2}$ at low temperatures) is relevant.

To identify the interaction responsible for the relaxation, we examine the magnitude of $T_1^{-1}$ at the maxima. Consider first the nuclear dipole-dipole interaction between neighboring $^7$Li nuclei. The strength of this interaction is measured by the Van Vleck second moment $(\Delta\omega_d^2)$.[12] Summing over the four nearest $^7$Li nuclei, we obtain $(\Delta\omega_d^2)^{1/2} \approx 2.5\times10^4$ sec$^{-1}$. Estimating the maximum relaxation at frequency $\omega$ from this interaction by $T_1^{-1}|_{max} \sim \Delta\omega_d^2/\omega$, we obtain ~5 sec$^{-1}$ at 21.5 MHz. This is too weak to explain the experimental value $\sim 5\times10^2$ sec$^{-1}$, which requires a stronger interaction. A time-varying component of the quadrupole interaction of magnitude $\Delta\omega_q \sim 2\times10^5$ sec$^{-1}$ would be sufficiently strong, but requires a high-temperature ratio $T_1/T_2 = 1$. The high-temperature data in Fig. 1 are in good agreement with a ratio of 4 and in clear disagreement with 1. Thus they support the dipolar interaction of Eq. (3). A nonzero time-averaged component of the quadrupole interaction is also required by the experimental ratio so that only the $\frac{1}{2} \leftrightarrow -\frac{1}{2}$ transition be observed, but evidently the quadrupole fluctuations $\Delta\omega_q$ are less than the above estimate. The source of the local field is evidently the dipole field of impurities with a magnetic moment, provided they are abundant enough to produce the observed magnitude of nuclear relaxation.

To check this proposed explanation, ESR signals have been searched for and found in our $Li_5AlO_4$ samples.[13] Resonances were observed at $g = 2.0$, 3.3, and 4.9. The $g = 2.0$ resonance is strongest, and is likely to be that of $Fe^{3+}$ ions in the $Al^{3+}$ positions. When the signal intensities were compared with that from a known amount of $CuCl_2 \cdot 2NC_5H_5$, the magnetic impurity concentration is estimated to be ~150 ppm per formula unit and hence per $Al^{3+}$. This corresponds to 15–20 ppm per cation site.

#### 1. Magnetic-impurity contributions to $T_1^{-1}$

Abragam[12] has discussed nuclear relaxation by magnetic impurities, and has shown that the dipolar interaction between the resonant nucleus and the impurity moment is more effective in producing relaxation than other interactions. The relaxation is determined by the time dependence of the impurity dipolar fields as seen by the nuclei, called the "local field." This time dependence is described by a correlation function which relates the local field at a given time with the local field at a time $t$ later. This is related to the component of the impurity moment in the direction of the magnetic field $S_z$ and is assumed to decay exponentially:

$$\langle\langle H_{loc}(0)\, H_{loc}(t)\rangle\rangle \propto \langle\langle S_z(0)\, S_z(t)\rangle\rangle \propto S(S+1)e^{-t/t_c} \quad (5)$$

For static lattices, the decay is due to longitudinal fluctuations of the impurity moment, and the correlation time $t_c$ is equal to the impurity $T_1$: $t_c = T_{1e}$. However if there is rapid motion of the $Li^+$ ions the decay will be due to $Li^+$ jumps, which occur within a time $\tau$, and $t_c = \tau \ll T_{1e}$. Implicit in our treatment which describes all the nuclei by a single correlation function (and neglects spin diffusion) is that the $Li^+$ diffusion is rapid enough that all the nuclei sample the same time-averaged environment within the experimental times $T_1$ and $T_2$ [$\langle\langle\ \rangle\rangle$ in Eq. (5) denotes a spatial and temporal average over all $^7$Li nuclei].

For this liquidlike model, Abragam's expression[12] [Eq. (40), p. 380], is slightly modified. For a powder, one obtains[14]

$$T_1^{-1} = \tfrac{2}{5} c\hbar^2\gamma_e^2\gamma_N^2 S(S+1)\frac{\tau}{1+\omega^2\tau^2}\sum_n \frac{1}{r_n^6}, \quad (6)$$

where $c$ is the impurity concentration, $\gamma_e$ and $\gamma_n$ are the impurity and nuclear gyromagnetic ratios, $S$ the impurity spin, and the sum is over neighboring $^7$Li nuclei at distances $r_n$ from the impurity. Assuming that the impurity is $Fe^{3+}$ ($S = \frac{5}{2}, g = 2.0$) and that it substitutes in an $Al^{3+}$ site, we calculate the sum (out to fourth neighbors) to be $3\times10^{46}$ cm$^{-6}$ for $\beta$-$Li_5AlO_4$. With 15-ppm $Fe^{3+}$, we calculate the maximum relaxation [$\omega\tau = 1$ in Eq. (6)] to be $T_1^{-1}|_{max} \approx 6\times10^2$ sec$^{-1}$ at 7.2 MHz. The nearly precise agreement with the experimental value is fortuitous, but demonstrates that the concentration of magnetic impurities observed with ESR is sufficient to explain our observed nuclear relaxation rates.

For thermally activated diffusion we expect

$$\tau = \tau_0 e^{E_a/kT}, \quad (7)$$

where $E_a$ is the thermal activation energy for a jump to occur and $\tau_0^{-1} \equiv \nu_0$ is usually identified as the jump attempt frequency. With this temperature dependence imposed on $\tau$ in Eq. (6), we expect three regimes of $T_1^{-1}$. At low temperatures $\omega^2\tau^2 \gg 1$, $T_1^{-1}$ increases with increasing temperature as $T_1^{-1} \propto \omega^2\tau^{-1}$. At $\omega\tau = 1$, $T_1^{-1}$ goes through a maximum. Finally at high temperatures $\omega^2\tau^2 \ll 1$, $T_1^{-1}$ decreases with increasing temperature as $T_1^{-1} \propto \tau$.

The $T_1^{-1}$ data in Fig. 1 above 136 °C show this behavior but with two minor differences. First, the frequency dependence below the maxima is slightly weaker than $\omega^{-2}$, being better described as $\sim\omega^{-1.8}$. Whether this is due to a minor frequency-independent contribution which we are unable to clearly identify, or whether the frequency dependence of the motion governed $T_1^{-1}$ is actually weaker than $\omega^{-2}$, we cannot say. The second deviation requires examination of the curves for each frequency at the maxima. The 7.2-MHz curve is more rounded than the 21.5-MHz curve, whereas Eq. (6) gives identically shaped curves displaced from each other. The rounding also results in a weaker than $\omega^{-1}$ frequency dependence of $T_1^{-1}$ at the maxima of the curves as predicted by Eq. (6).

Equation (7) can be used with the observed temperature of the $T_1^{-1}$ maxima to extract the attempt frequency. We take the observed activation energy to be the barrier height $E_a$ in (7). Using $E_a = 0.56$ eV, the 21.5-MHz data can be fit quite well with $\nu_0 = 2\times10^{12}$ sec$^{-1}$. The other frequencies and the uncertainty in $E_a$ give a factor of 2 uncertainty in this value.

### 2. *Magnetic-impurity contributions to $T_2^{-1}$*

The motional narrowing of $T_2^{-1}$ between 236 and 330 °C can be accounted for by the same model. In this temperature range, $T_2^{-1}$ is determined by low-frequency longitudinal fluctuations of the local field. We then expect Eq. (6) to also describe $T_2^{-1}$ if we let $\omega \to 0$ and divide by two (there is only one longitudinal local-field direction, whereas there are two independent transverse directions):

$$T_2^{-1}|_{\parallel} = \tfrac{1}{5} c\hbar^2\gamma_e^2\gamma_N^2 S(S+1)\tau \sum_n \frac{1}{r_n^6} . \tag{8}$$

If the $T_2^{-1}$ data in the above temperature range are extrapolated into the high-temperature region where $T_1^{-1} \propto \tau$, we find $T_1^{-1} \approx 1.7 T_2^{-1}|_{\text{extrap}}$, in fair agreement with the expected factor of 2. Above 330 °C, transverse fluctuations contribute significantly to $T_2^{-1}$, enhanced by a factor $\eta$ (= 7 for $I = \frac{5}{2}$) because we are only observing the $\frac{1}{2} \leftrightarrow -\frac{1}{2}$ nuclear transition

$$T_2^{-1} = T_2^{-1}|_{\parallel} + \tfrac{1}{2}\eta T_1^{-1} . \tag{9}$$

For isotropic relaxation in the high-temperature regime, i.e., for $T_2^{-1}|_{\parallel} = \frac{1}{2}T_1^{-1}$, the ratio $T_1/T_2 = (I+\frac{1}{2})^2$ is obtained as discussed in Sec. III.

Equation (8) and the above $T_2^{-1}$ data correspond to the high-temperature regime of the magnetic "tagging" experiments of Hogg *et al.*,[15] who doped the $F^-$ conductor $PbF_2$ with $Mn^{2+}$ impurities. Their data show a peak in $T_2^{-1}$, with the low-temperature regime being described by

$$T_2^{-1} \approx zc/\tau , \tag{10}$$

where $z$ is the number of neighboring $^7$Li sites which couple to the magnetic impurity. Equation (10) can be physically interpreted as being the rate at which nuclei encounter a strong local field which does not permit them to refocus and contribute to the spin echo. This mechanism should be appropriate for the magnetic impurity contribution to $T_2^{-1}$ in some region below 236 °C. However, we are not able to separate its contribution to the experimental value from that of the nuclear dipole-dipole interaction. If we assume that the correlation time for the nuclear-dipole interaction is the same as that obtained from $T_1^{-1}$, we can estimate $T_2^{-1}|_d \approx \Delta\omega_d^2\tau_c \sim 10^3$ sec$^{-1}$ at 100 °C. Thus while $T_2^{-1}|_d$ might obscure the magnetic contribution at lower temperatures, it is very unlikely to be influencing the experimental values above the 236 °C point, where $\tau_c$ has further decreased by two orders of magnitude. Since $T_2^{-1}|_d$ decreases with increasing temperature and Eq. (10) increases, adding the two may account for the nearly temperature-independent experimental values between 20 and 236 °C.

To find the approximate conditions of the maximum in the magnetic contribution to $T_2^{-1}$, we can equate (8) and (10) to obtain (approximated to first neighbors)

$$\tfrac{1}{5}\tau\hbar\gamma_e\gamma_N[S(S+1)/r_n^3] \sim 1 , \tag{11}$$

and

$$T_2^{-1}|_{\max} \sim \tfrac{1}{5} zc\hbar\gamma_e\gamma_N S(S+1) . \tag{12}$$

These expressions can be checked for consistency with the jump times obtained with the $T_1^{-1}$ analysis. At the onset of the exponential temperature dependence at 236 °C, we obtain a value of ~1.9 for the left-hand side of (11) and calculate $T_2^{-1}|_{\max} \sim 4\times10^3$ sec$^{-1}$, in fair agreement with the slightly peaked experimental value of $\sim10^4$ sec$^{-1}$. A complete theoretical treatment of $T_2^{-1}$ over the entire temperature range has recently been obtained.[14]

### B. Relaxation by magnetic fluctuations

At 86 °C and below, $T_1^{-1}$ deviates dramatically from its extrapolated temperature dependence in the range 150–250 °C. The frequency dependence is still observed, but the correlation time $t_c$ appears to be shorter than expected by assuming that (7) describes $t_c$ over the entire experimental temperature range. The temperature dependence of $t_c$ is also very weak.

A ready explanation of these features is provided with the magnetic impurity model by assuming that at ~100 °C, $\tau \sim T_{1e}$ so that at lower temperatures the correlation function decays by the more rapid fluctuations of the magnetic moment rather than $Li^+$ jumps. The $T_1^{-1}$ analyses and data below 100 °C thus allow us to estimate $T_{1e} \sim 1 \times 10^{-5}$ sec$^{-1}$ at room temperature. The room-temperature linewidth of the $g=2$ ESR resonance is ~8 Oe, which places an upper limit $T_{2e}^{-1} \lesssim 7 \times 10^7$ sec$^{-1}$. Since $T_{1e} \gtrsim T_{2e}$, we obtain $T_{1e} \gtrsim 1.4 \times 10^{-8}$ sec, which our value from the NMR analysis satisfies.

## V. $\alpha$-$Li_5AlO_4$ DATA AND ANALYSIS

$^7$Li nuclear relaxation rates were measured in $\alpha$-$Li_5AlO_4$ from 24 to 750 °C. Since differential thermal analysis show the onset of the $\alpha \rightarrow \beta$ transition at 780 °C, we limited ourselves to the above range of temperatures in order not to be troubled by the irreproducibility of results such as observed when metastable $\beta$-$Li_5AlO_4$ was heated too high. We checked and found that samples cycled to 750 °C and back to lower temperatures gave the same $T_1$ and $T_2$ values as previously obtained. $T_1^{-1}$ values obtained at 21.5, 12.7, and 7.2 MHz and $T_2^{-1}$ values at 21.5 MHz are shown in Fig. 2. Only a single component was detected in the nuclear relaxation curves, in agreement with x-ray analysis which showed only $\alpha$-$Li_5AlO_4$ to be present. Throughout the entire study, samples sealed as above showed no evidence of deterioration (such as discoloration or chemical attack of the quartz tube). With the known effects of water vapor on the conductivity in mind, we stress that our results are for pure $\alpha$-$Li_5AlO_4$ without water or LiOH contamination.

### A. Diffusive relaxation

In many respects the data in Fig. 2 resemble those of the metastable $\beta$ phase in Fig. 1. A diffusive regime is observed between 300–750 °C. The high-temperature ratio $T_1/T_2 \sim 4$ again requires relaxation by magnetic impurities. In this case, however, $T_1^{-1}|_{max} \propto \omega^{-1}$ as expected from (6), though the temperature position of the maximum changes

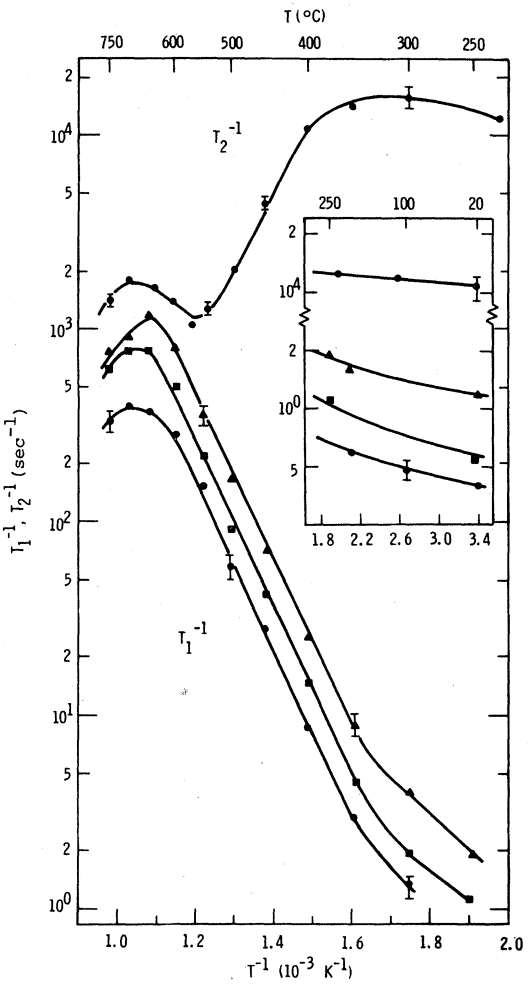


FIG. 2. Experimental values of $T_1^{-1}$ (●: 21.5 MHz, ■: 12.7 MHz, and ▲: 7.2 MHz) and $T_2^{-1}$ (●: 21.5 MHz) are given for the $^7$Li resonance in $\alpha$-$Li_5AlO_4$ for temperatures between 250–750 °C in the large graph, with 20–250 °C in the inset. Representative error limits are shown for selected points. The solid curves show experimental trends and are not theoretical fits to the data.

little with frequency, and the 750 °C values are not frequency independent. Qualitatively, in the $\alpha$ phase we apparently must go higher in temperature (650 °C) to obtain the same jump times at the maxima as with the metastable $\beta$ phase (400 °C). In the $\alpha$ phase, however, the frequency dependence below the maximum is approximately $\omega^{-1.0}$ vs $\omega^{-1.8}$ for the $\beta$ phase and $\omega^{-2.0}$ as expected from Eq. (6).

#### *1. Magnetic-impurity contributions to $T_1^{-1}$*

To check the effectiveness of relaxation by the magnetic impurities, we apply Eq. (6) to $\beta$-$Li_5AlO_4$ at 7.2 MHz. The sum over neighboring sites is

$4\times10^{46}$ cm$^{-6}$, giving $T_1^{-1}|_{max} \approx 9\times10^2$ sec$^{-1}$, which is comparable to the experimental value $1.2\times10^3$ sec$^{-1}$. Thus magnetic-impurity relaxation is sufficiently rapid to explain our data, and the following analyses closely parallel those of $\beta$-$Li_5AlO_4$.

Turning to the data between 300 and 750 °C, we find that $T_1^{-1}$ data for each frequency shown an activation energy $E_a = 0.83(2)$ eV. The temperature of each maximum can then be fit with the $\omega\tau \approx 1$ condition to obtain an attempt frequency. When the results from each frequency along with the uncertainty in $E_a$ are considered, we conclude $\nu_0 = 2\times10^{12}$ sec$^{-1}$ to within a factor of 2. We have ignored the weaker frequency dependence of the data, but we still expect the condition $\omega\tau \approx 1$ to hold in the vicinity of the maxima.

### 2. *Magnetic-impurity contributions to $T_2^{-1}$*

The activation energy of the $T_2^{-1}$ data in the motional narrowing regime 400–550 °C is approximately the same [0.78(8) eV] as that of the $T_1^{-1}$ data. Extrapolating these data into the high-temperature $T_1^{-1}$ regime gives $T_1^{-1} \approx 1.4T_2^{-1}|_{extrap}$, in fair agreement with Eqs. (6) and (8). The data show a slight peak at 300–350 °C whose magnitude is within a factor of 3 of that calculated above from Eq. (12). However, we calculate a value of ~40 for the left-hand side of Eq. (11). Thus the $\alpha$-phase data are not as consistent with the model for magnetic-impurity relaxation given in Sec. IV A as are the $\beta$ data. The poor agreement with Eq. (11) suggests that our values of $\tau$ (and hence $\nu_0$ and $E_a$) extracted from the $T_1^{-1}$ data are less reliable.

### B. Relaxation by magnetic fluctuations

A break from the diffusive regime to a much more slowly temperature-dependent $T_1^{-1}$ regime is seen again in Fig. 2 below 300 °C. As before, if we assume that at 300 °C $\tau \approx T_{1e}$, we estimate $T_{1e} \sim 2\times10^{-5}$ sec at room temperature. This again satisfies the ESR upper limit discussed in Sec. IV B, but is subject to the reliability of the $\tau$ value.

## VI. LiOH DATA AND ANALYSIS

Powdered samples of reagent grade LiOH were sealed in quartz tubes under a partial argon atmosphere. We attempted to work with both the $^7$Li and $^1$H resonances but were hampered by extremely long $T_1$ values, which limited how fast we could repeat the pulse sequence and accumulate data. For the $^7$Li resonance, the optimum repetition period at room temperature was ~200 sec, decreasing to ~1 sec at 430 °C. The corresponding values for the $^1$H resonance were 60 and 2 sec. With these unfavorable $T_1$ values, we chose to measure only $T_2^{-1}$ at 21.5 MHz. Shown in Fig. 3 are $T_2^{-1}$ values for both the $^1$H and $^7$Li resonances at room temperature and in the range 300–435 °C.

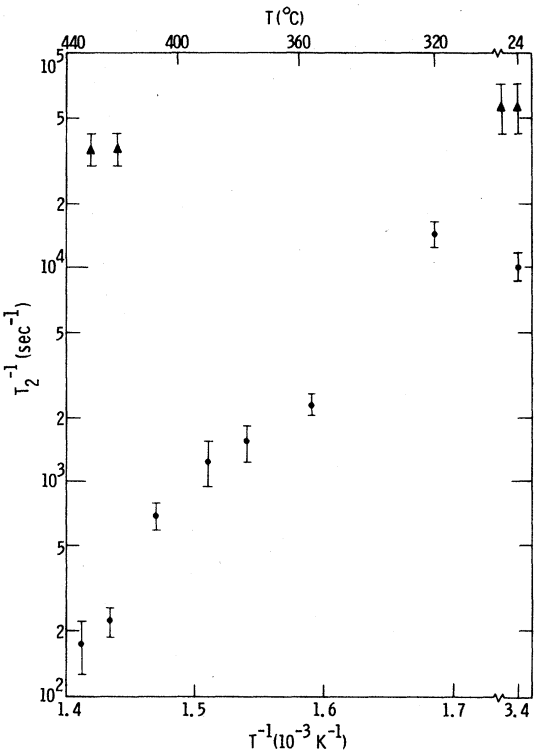


FIG. 3. $T_2^{-1}$ data for the $^7$Li resonance (●) and the $^1$H resonance (▲) in LiOH. Note that the horizontal (temperature) scale is broken at the far right to include room-temperature data.

The proton value evidently remains constant from 24 to 300 °C. It decreases only slightly at 430 °C, which is just below the melting temperature of 470 °C. The absence of motional narrowing shows that the protons are evidently static until just prior to melting, and are not responsible for the conductivity of LiOH. Proton relaxation is due to the nuclear dipole interaction, for which the onset of motional narrowing is described by[12]

$$\omega_d\tau_H \approx 1\,, \tag{13}$$

where $\omega_d$ is the static lattice dipole interaction and $\tau_H$ the proton jump time. Using the static lattice $T_2^{-1}$ value for $\omega_d$, the absence of motional narrowing then requires $\tau_H \gtrsim 3\times10^{-5}$ sec at 430 °C.

The $^7$Li data show clear evidence of $Li^+$ motion by the decrease in $T_2^{-1}$ above 320 °C. These data show more scatter than those of the previously discussed compounds but are in fair agreement

with a thermally activated mechanism with $E_a = 1.3(2)$ eV. $T_2^{-1}$ evidently exhibits a peak at 320 °C with the start of motional narrowing. This suggests that the interaction responsible for the diffusive relaxation is again magnetic impurities. While further data, especially $T_1^{-1}$, are needed for a more complete understanding of the nuclear relaxation processes in LiOH, our results definitely identify $Li^+$ as the diffusing ion.

## VII. DISCUSSIONS AND CONCLUSIONS

We turn now to exploring explanations for the deviations from the relaxation by magnetic impurities as discussed in Sec. IVA. The strongest deviations occur with the $\alpha$-$Li_5AlO_4$ data, especially the weak frequency dependence at temperatures below the $T_1^{-1}$ maxima ($T_1^{-1} \propto \omega^{-1}$ instead of $\omega^{-2}$). As a first explanation, we might try to separate the experimental rate into two contributions:

$$T_1^{-1} = A + B\omega^{-2}, \tag{14}$$

where $B\omega^{-2}$ is the magnetic impurity contribution to $T_1^{-1}$ and $A$ is a second frequency-independent contribution. The data between 300 and 600 °C can be fitted with such an expression. However, the resulting $A$ terms are strongly temperature dependent with an apparent activation energy which is about the same as that of the $B\omega^{-2}$ terms. Forcing the data to fit Eq. (14) therefore seems inappropriate since the frequency-independent contribution would also be apparently determined by the same $Li^+$ motion. The net effect of such a fit on the 7.2-MHz data is to increase $E_a$ slightly and double $\nu_0$.

As a check on our use of the liquidlike $Li^+$ diffusion model, we can require the ions to have adequate diffusion to encounter at least one impurity during $T_1$. This can be expressed mathematically as[14]

$$(6DT_1/a^2)c > 1, \tag{15}$$

where $a$ is the Li-Li jump distance, $c$ the impurity concentration, and $D$ the diffusion constant. We can estimate $D \approx \nu a^2$, where $\nu$ is the $Li^+$ jump rate, and then obtain

$$6\nu T_1 c > 1. \tag{16}$$

At the minimum $T_1 \approx 10^{-3}$ sec, $\nu \approx \omega = 4.5\times10^7$ $sec^{-1}$ (7.2 MHz), and for $c = 15\times10^{-6}$ we obtain $6\nu T_1 c = 4.0 > 1$. Approximately this value is appropriate over the entire diffusion regime since on the low-temperature side $T_1 \propto \nu^{-1}$. However in the magnetic fluctuation regime $T_1$ is shorter than predicted by $\nu^{-1}$. At room temperature for $\beta$-$Li_5AlO_4$ we obtain $6\nu T_1 c \sim 0.1$, while an even less staisfactory value is obtained for $\alpha$: $6\nu T_1 c \sim 10^{-4}$, thus questioning the $Li^+$ diffusion model in the magnetic fluctuation regime, especially for $\alpha$.

If $Li^+$ diffusion is too slow, we might expect that a spin-diffusion model is appropriate. In this case, the diffusion rate is given by $6D/a^2 \approx T_2^{-1} \approx 10^4$ $sec^{-1}$, where the rigid lattice $T_2$ is used to estimate the time for mutual spin flips. If this value satisfies Eq. (15), then Eq. (6) still remains valid. However at room temperature $T_1 \sim 1$ sec, and we obtain $6DT_1 c/a^2 \approx 0.2$, which questions the use of (6). For $6DT_1 c/a^2 \ll 1$, the slow diffusion treatment of Abragam[12] gives (for $\omega T_{1e} \gg 1$)

$$T_1^{-1} \propto \omega^{-1/2} T_{1e}^{-1/4}. \tag{17}$$

This gives a weak temperature dependence (through $T_{1e}$), and the magnitude calculated with Abragam's full expression [Eq. (44), p. 382] is in fair agreement with our room-temperature values. However, the frequency dependence is weaker than our observed $T_1^{-1} \sim \omega^{-1}$. It is possible that we are in an intermediate diffusion regime where neither (6) nor (17) is appropriate. A further complication is the spin-diffusion barrier[16] which has not been accounted for in (17).

Two modifications of relaxation equations similar to (6) have been proposed to account for weaker frequency dependences. First, we consider that of Walstedt *et al.*,[17] used to explain $T_1$ data for the $^{23}Na$ resonance in Na $\beta$-alumina. Their explanation proposes that there is not just a simple single-valued energy barrier to be overcome in the diffusion process, but a distribution of activation energies due to imperfections with the crystal lattice. This model changes the frequency dependence at and just below the $T_1^{-1}$ maximum essentially by spreading the $\omega^{-1}$ dependence of the maximum over a range of temperatures in which different components of the energy distribution are going through the $\omega\tau \approx 1$ condition. Such a distribution might explain the frequency dependence of the $T_1^{-1}$ maxima in $\beta$-$Li_5AlO_4$, but not the $\omega^{-1}$ dependence in $\alpha$-$Li_5AlO_4$ away from the maximum.

The second possible explanation assumes that there are more than one type of crystographically different sites for $Li^+$ occupation, with different energy barriers to be overcome and different thermal equilibrium populations. The discussion in Sec. II shows this could readily be the case for $Li_5AlO_4$. Several workers have modeled relaxation for such cases.[18,19] In such models, the thermal average occupation of the higher-energy site ($P = pe^{-\Delta/kT}$) multiplies an expression like Eq. (6) to give $T_1^{-1}$. One then obtains an activation energy $E_a + \Delta$ on the low-temperature side of the $T_1^{-1}$ maximum and $E_a - \Delta$ on the high-temperature side.

Equation (8) for $T_2^{-1}$ would also be multiplied by $P$ and have a net activation energy $E_a - \Delta$. However, our $T_2^{-1}$ and $T_1^{-1}$ data show essentially the same activation energy, and thus do not fit this proposed explanation.

None of the possible explanations considered above is able to explain deviations from (6) observed in our data. The data thus remain as tests for theories of magnetic impurity relaxation in ionic conductors and of detailed $Li^+$ motion in $Li_5AlO_4$. The frequency dependence of $T_1^{-1}$ and the diffusivity estimates suggest that the simple rapid-diffusion approach is less appropriate for $\alpha$-$Li_5AlO_4$, and that the jump parameters we have obtained for it are less reliable. A more general treatment utilizing both particle and spin diffusion for all values of the ratio $\tau/T_{1e}$ is currently in progress.[14]

Our $T_1^{-1}$ and $T_2^{-1}$ measurements have shown thermally activated $Li^+$ motion in all the materials studied. The activation energy of $\alpha$-$Li_5AlO_4$ [0.83(2) eV] is comparable to values obtained from recent conductivity measurements [0.94(4) eV] on samples without LiOH contamination which were either in vacuum or under argon.[20] We note that in principle our NMR activation energy need not agree with that of conductivity measurements since the correlation function [Eq. (5)] involves $Li^+$ jumps into and away from neighboring sites to magnetic impurities, while the conductivity is determined by jumps in the bulk material. The impurities could change the energy of neighboring sites and produce a different activation energy for nuclear relaxation. The attempt frequency, $2 \times 10^{12}(\times/\div 2)$ $sec^{-1}$, is close to a typical phonon frequency ($\sim 10^{13}$ $sec^{-1}$) and is not anomalously low like values observed in several other ionic conductors.[21]

We have shown that low concentrations of magnetic impurities in nominally pure ionic conductors can produce nuclear relaxation rapid enough to be the dominant relaxation mechanism. For $I \neq \frac{1}{2}$ nuclei, however, a second possible rapid relaxation mechanism is the electric quadrupole interaction. We emphasize that the correct mechanism can be identified by the ratio of $T_1/T_2$ at high temperatures when only the central nuclear transition is being observed. The former gives $(I+\frac{1}{2})^2$, while the latter gives a ratio $\frac{1}{4}$ as large. For $I = \frac{3}{2}$, the quadrupole ratio has the value of 1, and thus cannot be distinguished from the case where all nuclear transitions are in communication with each other. The nuclear dipole-dipole interaction gives a ratio ($= 1.4$ for $I = \frac{3}{2}$) close to that of quadrupole interactions,[10] but can likely be removed from consideration by its weaker contribution to $T_1^{-1}$. However, an experimental ratio of 4 clearly identifies magnetic impurities. This appears to be the case for the $^7Li$ resonances in the ionic conductors $Li_2Ti_3O_7$ [Ref. (21)] and $\beta$-$LiAlSiO_4$ [Ref. (22)]. The $^{63}Cu$ resonance in CuI [Ref. (23)] yields a ratio of 1, and its relaxation mechanism has been analyzed with the electric quadrupole interaction. Finally, the transition from a thermally activated $T_1^{-1}$ at high temperatures to a weakly temperature-dependent $T_1^{-1}$ at lower temperatures (where we have argued $t_c \approx T_{1e}$) may be expected in other systems with magnetic impurities, provided other relaxation mechanisms (for example, phonons) do not obscure it.

## ACKNOWLEDGMENTS

We wish to thank B. R. Hansen for capably performing the nuclear relaxation measurements. We are grateful to P. Richards for valuable discussions about the high-temperature $T_1/T_2$ ratio and relaxation by magnetic impurities. We thank E. Venturini for making the ESR information available to us. This work was supported by the

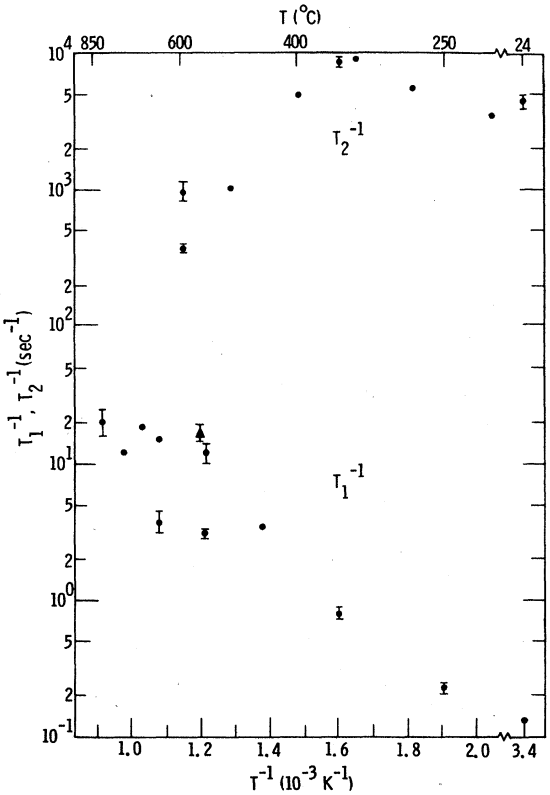


FIG. 4. $T_1^{-1}$ and $T_2^{-1}$ data for the $^7Li$ resonance in $\gamma$-$LiAlO_2$ at 21.5 MHz (●) with one datum at 12.7 MHz (▲). Representative error limits are shown for selected points. Note that the horizontal (temperature) scale is broken at the far right to include room-temperature data.

United States Department of Energy, DOE, under Contract No. AT(29-1)789, at Sandia Laboratories, a U. S. Department of Energy facility.

## APPENDIX

We report here the results of $T_1^{-1}$ and $T_2^{-1}$ measurements on $\gamma$-$LiAlO_2$. As with the other systems studied here, samples were sealed in quartz tubes under a partial argon atmosphere. With the exception of one datum, the results shown in Fig. 4 were obtained at 21.5 MHz.

$T_2^{-1}$ shows a slight peak just prior to the onset of motional narrowing at ~350 °C, again suggesting relaxation by magnetic impurities. On heating to ~600 °C, two components are detected in the transverse magnetization decay curve.

$T_1^{-1}$ begins to rapidly increase above 300 °C. At 550 and 650 °C two components were also found in the longitudinal magnetization relaxation curves. Thus at temperatures above 550 °C, both $T_1^{-1}$ and $T_2^{-1}$ show evidence of two distinct groups of $Li^+$ ions in $\gamma$-$LiAlO_2$. While the motional narrowing indicates definite $Li^+$ motion, a given $^7Li$ nucleus is evidently largely confined to one of two groups of sites. If a given nucleus samples all types of $Li^+$ sites during the relevant experimental times, we would expect a single-component relaxation curve, representing a sample-averaged value of $T_1^{-1}$. The long $T_1$ value at 550–650 °C shows that motion between the two groups of sites is slower than ~3 sec. Our results do not mean that there are not two groups of sites at lower temperatures, but if so the relaxation rates are too close to each other to separate. When they differ by ~×3 as for the data above 550 °C, two distinct rates can be resolved.

The smaller $T_2^{-1}$ and larger $T_1^{-1}$ components appear to be associated with $Li^+$ diffusion with an activation energy of 0.60 eV. Expecting perhaps a maximum in $T_1^{-1}$, we measured the larger $T_1^{-1}$ component up to 824 °C. Instead, we found a nearly constant $T_1^{-1}$ value from 550–824 °C. We cannot be absolutely certain that these results were not influenced by the second $T_1^{-1}$ component. A frequency check of the larger $T_1^{-1}$ component at 560 °C and 12.7 MHz showed little if any frequency dependence.

We emphasize that a more complete and careful study of both components of $T_1^{-1}$ and $T_2^{-1}$ is needed to better understand $Li^+$ diffusion in $\gamma$-$LiAlO_2$ and to confirm or dispell the above tentative analysis.

[1]I. D. Raistrick, C. Ho, and R. A. Huggins, Mater. Res. Bull. 11, 953 (1976).
[2]R. T. Johnson, Jr., R. M. Biefeld, and J. D. Keck, Mater. Res. Bull. 12, 577 (1977).
[3]F. Stewner and R. Hoppe, Z. Anorg. Allg. Chem. 380, 241 (1971).
[4]F. Stewner and R. Hoppe, Z. Anorg. Allg. Chem. 381, 149 (1971).
[5]R. Hoppe and H. Konig, Z. Anorg. Allg. Chem. 430, 211 (1977).
[6]F. Stewner and R. Hoppe, Acta Crystallogr. B 27, 616 (1971).
[7]E. R. Andrew and D. P. Tunstall, Proc. Phys. Soc. 78, 1 (1961).
[8]W. W. Simmons, W. J. O'Sullivan, and W. A. Robinson, Phys. Rev. 127, 1168 (1962).
[9]R. E. Walstedt, Phys. Rev. Lett. 19, 146 (1967); 19, 816(E) (1967).
[10]P. A. Fedders, Phys. Rev. B 13, 2768 (1976).
[11]N. Bloembergen, E. M. Purcell, and R. V. Pound, Phys. Rev. 73, 679 (1948).
[12]A. Abragam, *The Principles of Nuclear Magnetism* (Oxford U.P., Oxford, England, 1961).
[13]E. Venturini (private communication).
[14]P. Richards (private communication).
[15]R. D. Hogg, S. P. Vernon, and V. Jaccarino, Phys. Rev. Lett. 39, 481 (1977).
[16]W. E. Blumberg, Phys. Rev. 119, 79 (1960).
[17]R. E. Walstedt, R. Dupree, J. P. Remeika, and A. Rodriguez, Phys. Rev. B 15, 3442 (1977).
[18]J. E. Andersen, J. Magn. Reson. 11, 398 (1973).
[19]M. Polak and D. C. Ailion, J. Chem. Phys. 67, 3029 (1977).
[20]R. M. Biefeld and R. T. Johnson (unpublished).
[21]B. A. Huberman and J. B. Boyce, Solid State Commun. 25, 759 (1978).
[22]H. T. Weaver (private communication).
[23]J. B. Boyce and B. A. Huberman, Solid State Commun. 21, 31 (1977).